Amino Acid Replacements at the H_2-Activating Site of the NAD-Reducing Hydrogenase from *Alcaligenes eutrophus*†

Christian Massanz and Bärbel Friedrich*

Institut für Biologie, Humboldt-Universität zu Berlin, Chausseestrasse 117, D-10115 Berlin, Germany

Received April 7, 1999; Revised Manuscript Received August 3, 1999

ABSTRACT: The role of amino acid residues in the H_2-activating subunit (HoxH) of the NAD-reducing hydrogenase (SH) from *Alcaligenes eutrophus* has been investigated by site-directed mutagenesis. Conserved residues in the N-terminal L1 (RGxE) and L2 ($RxCGxCx_3H$) and the C-terminal L5 ($DPCx_2Cx_2H/R$) motifs of the active site-harboring subunit were chosen as targets. Crystal structure analysis of the [NiFe] hydrogenase from *Desulfovibrio gigas* uncovered two pairs of cysteines (motifs L2 and L5) as coordinating ligands of Ni and Fe. Glutamate (L1) and histidine residues (L2 and L5) were proposed as being involved in proton transfer [Volbeda, A., Charon, M.-H., Piras, C., Hatchikian, E. C., Frey, M., and Fontecilla Camps, J. C. (1995) *Nature 373*, 580−587]. The *A. eutrophus* mutant proteins fell into three classes. (i) Replacement of the putative four metal-binding cysteines with serine led to the loss of H_2 reactivity and blocked the assembly of the holoenzyme. Exchange of Cys62, Cys65, or Cys458 was accompanied by the failure of the HoxH subunit to incorporate nickel, supporting the essential function of these residues in the formation of the active site. Although the fourth mutant of this class (HoxH[C461S]) exhibited nickel binding, the modified protein was catalytically inactive and unable to oligomerize. (ii) Mutations in residues possibly involved in proton transfer (HoxH[E43V], HoxH[H69L], and HoxH[H464L]) yielded Ni-containing proteins with residual low levels of hydrogenase activity. (iii) The most promising mutant protein (HoxH[R40L]), which was identified as a metal-containing tetrametric enzyme, was completely devoid of H_2-dependent oxidoreductase activity but exhibited a remarkably high level of D_2-H^+ exchange activity. These characteristics are compatible with the interpretation of a functional proton transfer uncoupled from the flow of electrons.

Hydrogenases, which are abundant among microorganisms, catalyze the reversible cleavage of H_2 into $2H^+$ and $2e^-$. On the basis of their metal content, two major classes of proteins are distinguished, [Fe] and [NiFe] hydrogenases. The more common [NiFe] hydrogenases consist of a large approximately 60 kDa subunit and a small 30 kDa subunit. The large subunit contains a heterodinuclear NiFe center, and the small subunit harbors one to three Fe−S clusters. It is generally accepted that H_2 activation occurs at the NiFe center and that the Fe−S clusters mediate electron transfer between the active site and redox partners such as cytochromes and ferredoxins (revieved in refs *1* and *2*).

The Gram-negative bacterium *Alcaligenes eutrophus* (renamed *Ralstonia eutropha*) is able to use molecular hydrogen as a sole source of energy for the synthesis of cell carbon from CO_2 (reviewed in ref *3*). Energy-linked H_2 oxidation in this bacterium is catalyzed by two [NiFe] hydrogenases. The membrane-bound hydrogenase (MBH)[1] is composed of a large subunit and a small subunit which are coupled to the electron transport chain via a cytochrome *b*-type anchor (*4*, *5*). The second hydrogenase (SH) of *A. eutrophus* is soluble and resides in the cytoplasm, where it reacts with NAD as the physiological electron acceptor (*6*). The SH is composed of two dimeric modules; the HoxH subunit with the NiFe center forms together with HoxY the hydrogenase unit (*7*−*9*). The NADH oxidoreductase module (diaphorase) consists of HoxF and HoxU and contains several not completely defined Fe−S clusters, in addition to one FMN and the NAD binding site. This Fe−S flavoprotein is closely related to the NADH:ubiquinone oxidoreductase of mitochondria and bacterial species (reviewed in refs *10* and *11*). The SH and MBH proteins of *A. eutrophus* are encoded by the genes *hoxFUYH* and *hoxKG*, respectively, which are arranged in two separate operons located on the 450 kb megaplasmid pHG1 (*12*, *13*).

Alignment of more than 70 primary sequences of [NiFe] hydrogenases revealed five consensus motifs in the Ni-containing large subunit: RGxE (L1), $RxCGxCx_3H$ (L2), Hx_6L (L3), Gx_4PRGx_3H (L4), and $DPCx_2Cx_2H/R$ (L5) (*1*, *14*). In [NiFeSe] hydrogenases, the first cysteine of the L5 motif is replaced with selenocysteine, which was identified as a ligand of the Ni ion in hydrogenases from *Desulfovibrio baculatus* (*15*) and *Methanococcus voltae* (*16*). The first crystallographic analysis of the periplasmic [NiFe] hydrogenase of *Desufovibrio gigas* showed that the active site is deeply buried inside the protein and that Ni and Fe are

† This work was supported by grants from Deutsche Forschungsgemeinschaft (Fr 305/11-1) and Fonds der Chemischen Industrie. A short-term scientific mission of C.M. to the laboratory of V. M. Fernàndez was funded by the European Commission Cooperation in Science and Technology, Action 818.

* Corresponding author. Telephone: ++49-30-20938100. Fax: ++49-30-20938102. E-mail: baerbel=friedrich@biologie.hu-berlin.de.

[1] Abbreviations: SH, soluble (cytoplasmic) hydrogenase; MBH, membrane-bound hydrogenase.

10.1021/bi9908080 CCC: $18.00
Published on Web 10/05/1999

Table 1: Bacterial Strains and Plasmids

	relevant characteristics	source or ref
strain		
A. eutrophus		
H16	SH^+ MBH^+ [a]	DSM 428, ATCC 17699
HF371	SH^- MBH^-,*hoxH*Δ, *hoxG*Δ	*29*
HF387	SH^- MBH^+, Δ(*hoxFUYHW*)	*29*
HF442	*hoxH*[TGC → AGC (C458S)]	this study
HF443	*hoxH*[TGC → AGC (C461S)]	this study
E. coli		
S17-1	*recA pro thi hsdR chr*::RP4-2 Tra^+	*30*
plasmid		
pBluescript KS+	*l*Ap^r*lacZ*′ T7 ϕ10 promoter f1*ori*	Stratagene, cloning system
pLO1	Km^r*sacB* RP4 *oriT* ColE1*ori*	*31*
pCH472	1.9 kb *Sst*I fragment of pGE15 in pBluescript KS+	*29*
pCH570	1.9 kb *Sst*I fragment of pGE289[b] in pLO1	this study
pCH571	1.9 kb *Sst*I fragment of pGE290[b] in pLO1	this study
pGE15	15.0 kb *Hin*dIII fragment of pHG1 in pVK101	*12*
pGE331	derivative of pGE15 with a 1.9 kb *Sst*I fragment deleted	*29*

[a] SH, soluble hydrogenase; MBH, membrane-bound hydrogenase. [b] Listed in Table 2.

bridged by two cysteine thiolates of the L2 and L5 motifs. The remaining thiolates of both cysteine pairs are monodentate ligands to the Ni atom. Moreover, the Fe coordinates three additional diatomic ligands (*17*, *18*). Very similar protein structures have been obtained for the [NiFe] hydrogenases from other *Desulfovibrio* species (*19*, *20*). Fourier transform infrared (FTIR) spectroscopy identified the diatomic ligands as one CO and two CN^- molecules (*21*−*23*). FTIR bands characteristic of these ligands were also identified in [NiFe] hydrogenases from other organisms, including *A. eutrophus* (*24*). Despite individual characteristics of the H_2 active site in the various [NiFe] hydrogenases, spectroscopic similarities and conservation of potential metal ligands are consistent with an overall conservation of the structure and function of the NiFe center. Moreover, the X-ray data of the crystallized hydrogenases showed that the small electron-transferring subunit is composed of two domains. The N-terminal domain harbors one [4Fe-4S] cluster proximal to the NiFe center. The C-terminal domain of the small subunit contains one [3Fe-4S] and one [4Fe-4S] cluster, and its tail obviously docks the enzyme to an electron acceptor (*17*−*20*). An equivalent electron-transferring function is assigned to HoxY, the small hydrogenase subunit of the SH from *A. eutrophus*. Its primary structure predicts a truncated protein bearing only the N-terminal domain with the proximal [4Fe-4S] cluster (*12*, *25*).

Despite an enormous wealth of structural information about [NiFe] hydrogenases, the precise role of Ni, Fe, and their associated ligands in H_2 catalysis is still a matter of debate (*2*, *26*, *27*). Early hydrogen−isotope exchange experiments showed that H_2 cleavage occurs heterolytically, yielding H^+ and H^- (*28*). Most of the [NiFe] hydrogenases undergo reductive activation before H_2 turnover occurs, but again, the underlying molecular mechanisms are scarcely known (*1*).

Application of genetic techniques in the analysis of hydrogenase catalysis has been hampered by the failure to express active hydrogenase heterologously in *Escherichia coli* and by deficiencies in appropriate systems for those organisms whose hydrogenases are biochemically and structurally well characterized. Although X-ray structure data are not yet available for the SH of *A. eutrophus*, this enzyme offers the following advantages. The biochemical properties are well defined; its maturation pathway is less complex than that of membrane-bound or periplasmic proteins, and its host is easily accessible to standard genetic manipulations. To gain insights into the function of the catalytic site, we generated a set of point mutations in the gene encoding HoxH and characterized the resulting mutant proteins with respect to enzymatic properties, Ni content, and structural composition.

EXPERIMENTAL PROCEDURES

Bacterial Strains and Growth Conditions. The bacterial strains and plasmids used in this study are listed in Table 1. Strains carrying the initials HF are derivatives of *A. eutrophus* H16 which harbors the endogenous megaplasmid pHG1. *E. coli* S17-1 (*30*) was used as a host in standard cloning procedures and was the donor in conjugative plasmid transfer.

Strains of *A. eutrophus* were cultivated in mineral salts medium containing 0.4% (w/v) fructose or a mixture of 0.2% (w/v) fructose and 0.2% (v/v) glycerol (FGN medium) (*32*). The standard medium was supplemented with 1 μM $NiCl_2$. Lithoautotrophic cultures were grown on mineral salts medium under an atmosphere of hydrogen, carbon dioxide, and oxygen (8:1:1, v/v/v). Strains of *E. coli* were grown in Luria-Bertani medium (*33*). Antibiotics were supplemented as follows: 350 μg of kanamycin per milliliter and 15 μg of tetracycline per milliliter for *A. eutrophus* and 25 μg of kanamycin per milliliter, 15 μg of tetracycline per milliliter, and 100 μg of ampicillin per milliliter for *E. coli*.

Recombinant DNA Techniques and Plasmid Constructions. Standard DNA techniques were used (*34*). Site-directed mutations in *hoxH* were constructed by a two-step PCR method (*35*). *hoxH* of pGE15 was subcloned into pBluescript KS+, yielding pCH472. Plasmid pCH472 served as a template, and *Taq* polymerase was used for DNA amplification. Mutations located at the 5′ end of *hoxH* were introduced by recombination of a 198 bp *Sty*I−*Bst*EII fragment into pCH472. Likewise, mutations located at the 3′ end of *hoxH* were introduced on a 98 bp *Bsm*I−*Bsm*AI fragment into pCH472. Codon changes and the resulting plasmids are listed in Table 2. Mutations were verified by double-stranded sequencing of the inserted DNA.

The broad-host-range plasmid pGE331 (Table 1) was derived from pGE15 by deletion of *hoxH* contained on a

Table 2: Mutant *hoxH* Alleles in Derivatives of pGE15[a]

plasmid	pBluescript cloning intermediate	codon change	amino acid change
pGE332	pCH475	CGG → CTG	R40L
pGE333	pCH476	GAA → GTA	E43V
pGE334	pCH477	CGC → CTC	R60L
pGE335	pCH478	TGC → AGC	C62S
pGE336	pCH479	TGT → AGT	C65S
pGE337	pCH480	CAC → CTC	H69L
pGE338	pCH481	TGC → GCC	C72A
pGE339	pCH482	GAT → GTT	D456V
pGE289	pCH388	TGC → AGC	C458S
pGE290	pCH390	TGC → AGC	C461S
pGE340	pCH483	TGC → AGC, TGC → AGC	C458S/C461S
pGE341	pCH484	CAC → CCA	H464L

[a] The characteristics of pGE15 are described in Table 1.

1.9 kb *Sst*I fragment. To generate recombinant plasmids for complementation studies, the modified *hoxH* alleles were inserted as a 1.9 kb *Sst*I fragment into pGE331 (Table 2). The mobilizable plasmids were transferred from *E. coli* S17-1 cells to SH-deficient *A. eutrophus* HF387 cells (Table 1) by a spot mating technique (*36*). Transconjugants were selected on minimal medium containing fructose and the appropriate antibiotics.

Two of the 12 *hoxH* mutant alleles were introduced into the endogenous megaplasmid pHG1 of *A. eutrophus* H16 to generate the isogenic strains HF442 and HF443 (Table 1). This was achived by inserting the corresponding 1.9 kb *Sst*I fragments of pCH388 and pCH390, respectively, into pLO1 and using the recombinant plasmids for allelic exchange with *A. eutrophus* H16 (*31*). Isolates were verified by PCR and restriction analysis.

Preparation of Soluble and Membrane Extracts. *A. eutrophus* cells were grown in FGN medium to an optical density of 10−11 at 436 nm. Cells were harvested by centrifugation, washed once, and resuspended in 50 mM potassium phosphate buffer (pH 7) containing 0.1 mM phenylmethanesulfonyl flouride. Cells were disrupted by two passages through a French pressure cell at 119 MPa, and soluble and membrane fractions were prepared as described previously (*32*). Protein concentrations were determined by the method of Lowry et al. (*37*) with bovine serum albumin as the reference.

Autoradiography of ^{63}Ni-Labeled Proteins. Proteins were labeled in vivo by growing the cells to an optical density of 10−11 at 436 nm in FGN medium containing 150 nM $^{63}NiCl_2$ (867 mCi/mmol; Amersham Buchler). Soluble extracts were analyzed by native PAGE and autoradiography as described previously (*38*).

Immunoblot Analysis. Proteins were separated by electrophoresis in polyacrylamide gels and transferred to BA83 nitrocellulose membranes (Schleicher and Schuell) according to a standard protocol (*39*). Subunits of the SH were detected with rabbit polyclonal antisera and an alkaline phosphatase-labeled goat anti-rabbit immunoglobuin (Jackson Immuno Research Laboratories). The antisera were prepared with individually isolated SH subunit proteins.

Enzyme Assays. Activities of the SH (hydrogen:NAD^+ oxidoreductase, EC 1.12.1.2) and the MBH (ferredoxin:H^+ oxidoreductase, EC 1.18.99.1) were determined with cells grown in FGN medium to an optical density of 10−11 at 436 nm. The hydrogenase activity of the SH was determined spectrophotometrically in soluble extracts by assessing the H_2-dependent reduction of NAD and benzyl viologen (BV). Diaphorase activity was assayed with the soluble fraction using BV as the acceptor and NADH as the electron donor (*6*). Deuterium−water (D_2−H_2O) exchange experiments were carried out as described previously (*29*).

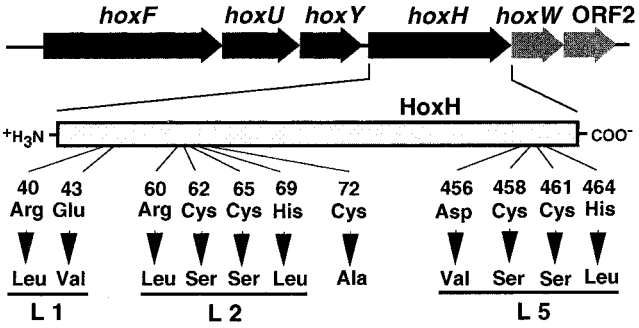

FIGURE 1: Replacement of selected amino acids in active site-containing subunit HoxH of the soluble hydrogenase. A simplified map displays the four SH structural genes *hoxF*, *-U*, *-Y*, and *-H* and two accessory genes *hoxW* and ORF2. The bar represents the HoxH protein. Numbers indicate the position of altered residues, and the replaced amino acids are listed below. The conserved motifs L1, L2, and L5 were adopted from Albracht (*1*).

RESULTS

Effect of Amino Acid Replacements in the Active Site-Containing Subunit HoxH on Lithoautotrophic Growth. The SH structural genes *hoxF*, *hoxU*, *hoxY*, and *hoxH* are clustered on megaplasmid pHG1 of *A. eutrophus* (*12*) together with the carboxyl-terminal protease gene *hoxW* and an open reading frame of unknown function (*40*). This gene cluster had been cloned in plasmid pGE15 (Figure 1) which restored the SH activity in strain HF387 from which the SH structural genes had been removed (*29*). We used plasmid pGE15 for introducing mutated *hoxH* alleles (Table 2) and for expression of the mutated genes in the SH-deficient recipient HF387. Site-directed mutations were constructed in vitro. The target residues which were altered in the HoxH polypeptide are highlighted in Figure 1. The conserved pairs of cysteine residues in the L2 and L5 motifs were each replaced with serine. In addition, the nonconserved Cys72 was exchanged with alanine. Nonpolar leucine was selected for substitution of arginine and histidine residues. The polar amino acids aspartate and glutamate were each replaced with nonpolar valine.

To obtain a first estimate on the phenotypic effect of the various mutations, cells were cultivated autotrophically with H_2 as the sole source of energy. With the exception of a single strain [HF387(pGE338)], the majority of mutants exhibited a significant retardation of lithoautotrophic growth (Table 3). This phenotype is characteristic of strains whose growth is solely supported by the MBH, e.g., HF387. A mutation of the nonconserved Cys72 yielded wild-type like lithoautotrophic growth, pointing to an unimpaired function of both hydrogenases.

Catalytic Properties of the Modified Proteins. Normally, assays for hydrogenase activity are restricted to the use of redox dyes as electron carriers or the application of the oxidoreductase-independent D_2−H^+ exchange reaction (*41*).

Table 3: Lithoautotrophic Growth of Strains Bearing Mutated *hoxH* Alleles

strain[a]	relevant characteristics	growth[b]
HF387	SH^-, MBH^+	+
HF387(pGE15)	SH^+, MBH^+	++
HF387(pGE332)	HoxH[R40L], MBH^+	+
HF387(pGE333)	HoxH[E43V], MBH^+	+
HF387(pGE334)	HoxH[R60L], MBH^+	+
HF387(pGE335)	HoxH[C62S], MBH^+	+
HF387(pGE336)	HoxH[C65S], MBH^+	+
HF387(pGE337)	HoxH[H69L], MBH^+	+
HF387(pGE338)	HoxH[C72A], MBH^+	++
HF387(pGE339)	HoxH[D456V], MBH^+	+
HF387(pGE289)	HoxH[C458S], MBH^+	+
HF387(pGE290)	HoxH[C461S], MBH^+	+
HF387(pGE341)	HoxH[H464L], MBH^+	+

[a] pGE15 is described in Table 1. [b] ++, doubling time of approximately 3.8 h; +, doubling time between 6 and 8.9 h.

The SH of *A. eutrophus* offers the advantage of using, in addition to the standard protocols, NAD as the physiological electron acceptor. Moreover, NADH oxidation can be monitored as an enzymatic function of the diaphorase module (*8*, *9*).

The results of the mutant analysis are summarized in Table 4. All mutant proteins with the exception of the SH prepared from HF387(pGE338) exhibited a significant decrease in the rate of H_2-dependent reduction of both NAD and BV. The loss of H_2−acceptor-reducing ability correlated in most cases with the activity pattern obtained with the D_2-H^+ exchange assay (Table 4). A remarkably different behavior, however, was observed with a protein modified in Arg40 (HoxH-[R40L]) which exhibited D_2-H^+ exchange activity of the wild-type level but a complete lack of H_2−acceptor-reducing activity. Overall, the NADH−BV-reducing activity of the mutant proteins ranged between 51 and 92% of the wild-type level. The reduced diaphorase activity results from protein degradation (data not shown).

Structure of Mutant Proteins. Biosynthesis of [NiFe] hydrogenases is a complex process which involves a series of maturation steps required for the assembly of the NiFe center (*42*). Ni insertion into the SH of *A. eutrophus* depends on at least six *hyp* gene products (*38*, *43*). Moreover, 24 amino acids have to be proteolytically removed from the C-terminus of HoxH before subunit oligomerization can occur (*29*, *40*).

To investigate if mutations in *hoxH* affect the maturation process and the stability of the mutant proteins, immunological investigations by Western blot analysis were performed. Under denaturing conditions, the less mobile HoxH precursor can be distinguished from its mature form (*38*) which comigrates with the purified HoxH polypeptide as demonstrated in Figure 2A (lanes 1 and 2). The existence of the HoxH precursor in the wild-type strain HF387(pGE15) probably results from a rate-limiting maturation process due to a high level of SH gene expression (*29*). Four mutants (Figure 2A, lanes 6, 7, 10, and 11) exhibited an accumulation of the precursor, which correlated with a deficiency in Ni incorporation (Figure 3). We cannot exclude the possibility of nonspecific proteolysis by HoxW since the signals from fast-migrating HoxH are slightly distinct form those of the wild-type protein (Figure 2A, lanes 7, 10, and 11). The His69-modified protein of mutant HF387(pGE337) exhibited an increased instability (Figure 2A, lane 8). In the remaining mutant strains, the mature version of HoxH was the dominant form pointing to normal C-terminal proteolysis.

To determine if the subunits assembled properly to the holoenzyme, an immunological assay was conducted under nondenaturing conditions (Figure 2B). As expected, the wild type exhibited two signals, one typical of the tetramer and a second assigned to unassembled HoxH (Figure 2B, lanes 1 and 2). Oligomerization to the tetramer was prevented in strains carrying modifications in the L2 and L5 motifs of HoxH (Figure 2B, lanes 5−7 and 10−12). Exchange of the putative Ni coordinating Cys residues led to the occurrence of unassembled HoxH derivatives. Similar results were obtained with mutants altered in the adjacent Arg60 and Asp456 residues.

Ni Content of the Mutant Proteins. To investigate whether a correlation exists among the loss of catalytic activity (Table

Table 4: Activity and Structure of SH Subunits in Soluble Extracts of Wild-Type and Mutant *A. eutrophus* Strains[a,b]

	enzyme activity[c]						
	hydrogenase			diaphorase	enzyme structure		
relevant characteristics[b]	($H_2 \rightarrow$ NAD)	($H_2 \rightarrow$ BV)	(D_2-H^+)	(NADH $\rightarrow$ BV)	tetramer	processing of HoxH	Ni in HoxH
WT SH	100	100.0	100.0	100	+	+	+
SH^-	0	<0.5	<0.5	5	ND[d]	ND	ND
R40L	0	<0.5	110.0	83	+	+	+
E43V	4	5.0	5.0	77	+	+	+
R60L	0	<0.5	<0.5	57	−	+	+
C62S	0	<0.5	<0.5	61	−	+	−
C65S	0	<0.5	<0.5	51	−	−	−
H69L	1	2.0	8.0	65	+	+	+
C72A	88	82.0	nd[e]	92	+	+	+
D456V	0	<0.5	<0.5	62	−	−	(-)[f]
C458S	0	<0.5	<0.5	60	−	−	−
C461S	0	<0.5	<0.5	54	−	+	+
H464L	5	5.0	24.0	67	+	+	+

[a] Cells were grown in fructose/glycerol medium (Friedrich 81). [b] HF387(pGE15) is the wild-type (WT) strain, and HF387 is the SH-negative (SH^-) strain; for mutant strains, see Table 3. [c] Activities are given in percentages; values of strain HF387(pGE15) are taken as 100%. The maximum level of H_2-dependent NAD and BV reduction is 3.1 and 1.5 μmol of H_2 min^{-1} mg of $protein^{-1}$, respectively. The maximal D_2-H^+ exchange rate is 0.91 μmol of HD min^{-1} mg of $protein^{-1}$. The maximal level of NADH-dependent benzyl viologen (BV) reduction is 5.1 μmol of NADH min^{-1} mg of $protein^{-1}$. Values give the average of data from three independent experinents. The variation was less than 25%. [d] ND, not detectable. [e] nd, not determined. [f] A weak signal of ^{63}Ni was detected.

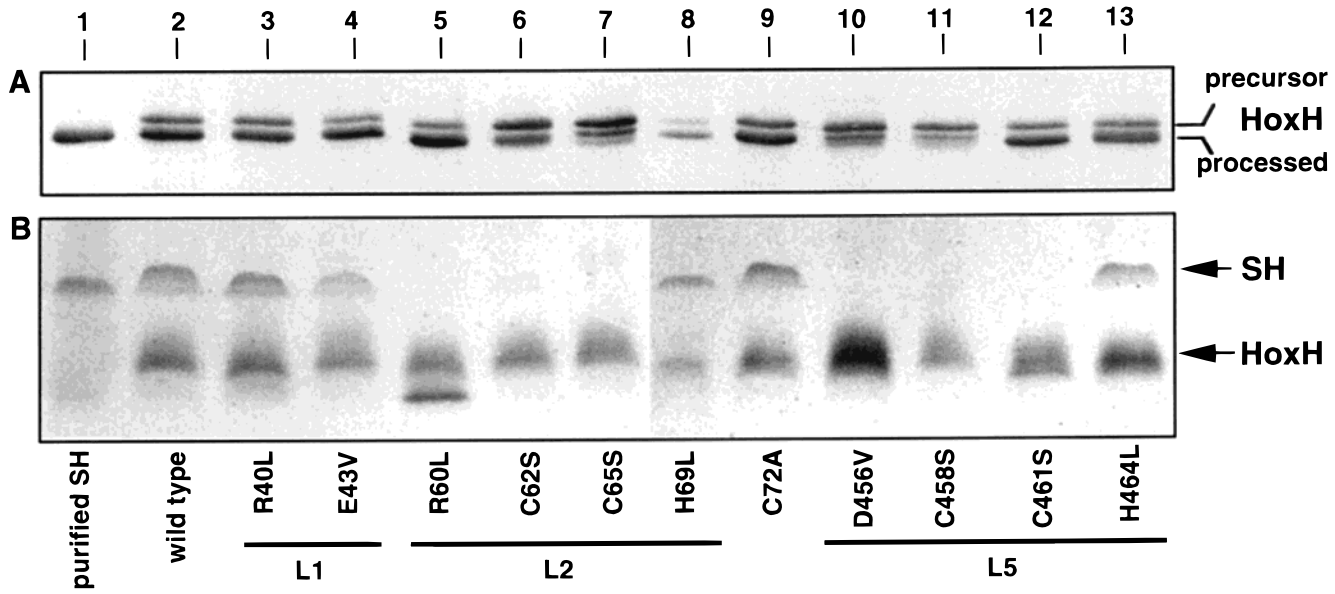

FIGURE 2: Western blot analysis of mutant extracts under denaturing (A) and nondenaturing conditions (B). Soluble extracts were separated on polyacrylamide gels, and HoxH-specific antibodies were used. (A) Soluble extracts (20 μg of protein) were applied to lanes 2−13 and separated by SDS−PAGE (12%): lane 1, 0.5 μg of purified SH; lane 2, HF387(pGE15); lane 3, HF387(pGE332); lane 4, HF387(pGE333); lane 5, HF387(pGE334); lane 6, HF387(pGE335); lane 7, HF387(pGE336); lane 8, HF387(pGE337); lane 9, HF387(pGE338); lane 10, HF387(pGE339); lane 11, HF387(pGE289); lane 12, HF387(pGE290); and lane 13, HF387(pGE341). (B) Soluble extracts (50 μg of protein) were applied to lanes 2−13 and separated by nondenaturing PAGE (gradient gel from 4 to 15%). Samples were applied as described for panel A.

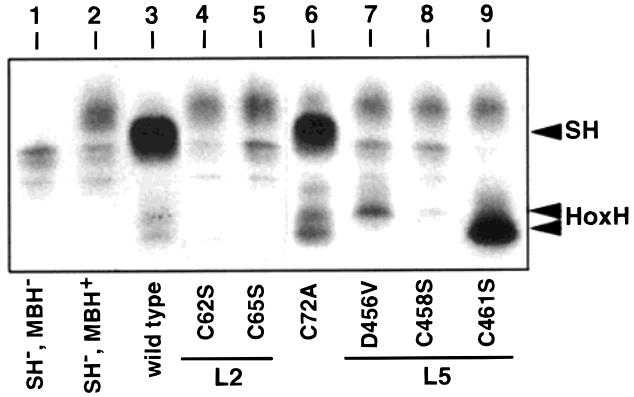

FIGURE 3: ^{63}Ni incorporation in vivo. Cells were grown in fructose/glycerol medium in the presence of 150 nM $^{63}NiCl_2$. A total of 100 μg of soluble extract was applied to each lane and separated by nondenaturing PAGE (gradient gel from 4 to 15%): lane 1, HF371; lane 2, HF387; lane 3, HF387(pGE15); lane 4, HF387(pGE335); lane 5, HF387(pGE336); lane 6, HF387(pGE338); lane 7, HF387(pGE339); lane 8, HF387(pGE289); and lane 9, HF387(pGE290).

4), the deficiency in maturation (Figure 2), and the absence of Ni, the mutants were cultivated under hydrogenase-derepression conditions in a medium supplemented with $^{63}NiCl_2$. Soluble extracts of these cells were separated by native PAGE, and Ni-labeled proteins were identified by autoradiography and Western blot analysis. Both techniques have been applied previously (*8*, *27*, *38*, *40*).

Of the five Cys-substituted mutants, only strain HF387-(pGE338), affected in the nonconserved Cys72, yielded an SH-specific Ni signal which was equivalent to the signal obtained with wild-type cells (Figure 3, lanes 3 and 6). Other Ni-labeled proteins, including the MBH, are demonstrated in the controls (lanes 1 and 2). Inspection of four mutants, altered in the putative Ni coordination residues Cys62, Cys65, Cys458, and Cys461, revealed absolutely no Ni signal in the L2 mutants (lanes 4 and 5), traces in the first L5 mutant (lane 8), and a remarkably intense signal in cells altered in the distal Cys461 residue (lane 9). The latter signal correlates with the immunologically identified HoxH subunit (data not shown). Exchange of Asp456, located close to the C-terminal pair of cysteine residues, yielded a weak Ni signal (lane 7) which indicates that this particular residue has a function in the assembly or structure of the NiFe center.

The mutant alleles *hoxH*[C458S] and *hoxH*[C461S] were also introduced into the endogenous megaplasmid of strain H16. The HoxH proteins of the resulting isogenic strains HF442 and HF443 exhibited the characteristics of the corresponding HoxH proteins from the transconjugants HF387(pGE289) and HF387(pGE390), respectively.

DISCUSSION

The mechanism of how the simplest molecule on earth, molecular hydrogen, is cleaved into protons and electrons is still a matter of debate, although three crystal structures of [NiFe] hydrogenases are available and more than 70 primary hydrogenase sequences have been deposited in the database. This wealth of information led to the identification of conserved structures in specific parts of the large subunit and the N-terminal region of the small subunit. A variable C-terminal domain docks the small subunit to the specific physiological acceptor (*1*). Moreover, a wide range of spectroscopic techniques have been applied to hydrogenases from various sources to obtain insights into their reaction mechanism. This is the first comprehensive report of directed mutagenesis focused on the catalytic site of [NiFe] hydrogenase. In previous studies, mutants of *Azotobacter vinelandii* (*44*) and *Desulfovibrio fructosovorans* (*45*) were generated with specific mutations in the gene for the electron-transferring small subunit and formerly isolated hydrogenase

mutants of *E. coli* hydrogenase 1 were only preliminarily characterized (*46*) without presenting data on the enzymatic function and the structural composition of the mutant proteins. Of the 11 mutants with amino acid exchanges in the soluble hydrogenase of *A. eutrophus*, 10 were hit in highly conserved residues which lie in the L1, L2, and L5 motifs of the HoxH subunit (Figure 1). Only a single nonconserved residue (Cys72) was selected as a mutational target yielding a mutant HoxH[C72A] protein with almost wild-type like properties.

Replacement of the two pairs of conserved cysteines, which have been recognized as coordinating the NiFe site in the enzymes crystallized so far (reviewed in ref *2*), resulted in nonoligomerized HoxH[C62S], HoxH[C65S], HoxH-[C458S], and HoxH[C461S] which were devoid of H_2-activating function irrespective of whether NAD and BV reduction or D_2-H^+ exchange activity was tested. Three of the four mutant proteins (HoxH[C62S], HoxH[C65S], and HoxH[C458S]) exhibited no incorporation of Ni. When the fact that Ni incorporation and C-terminal processing of the large subunit are tightly coupled processes is taken into account (*42*), it is not surprising that most of the Ni-free mutant HoxH proteins accumulated as precursors. However, it is remarkable that some of the HoxH[C62S] polypeptides appeared to be processed like the wild-type HoxH.

To our surprise, replacement of the distal Cys461, which correlates with the bridging ligand Cys533 in the crystallized *D. gigas* enzyme (Figure 4), still allowed C-terminal proteolysis of HoxH and Ni binding to this subunit. The fact that the HoxH[C461S] mutant protein was catalytically inactive and unable to form the tetramer suggests that proper folding of the enzyme does not occur. It is also possible that this mutant protein is trapped in a complex with Hyp proteins which are involved in the insertion of the active site (*38*, *43*). From the genetic approach, we conclude that Ni coordination in the soluble hydrogenase of *A. eutrophus* is in general agreement with the published crystal structures (*17*−*20*) which shows that the Ni ligands are arranged in a highly distorted square pyramidal conformation in which the distal cysteine occupies the axial position located opposite a vacant site. This axial ligand correlates with Cys461 in the HoxH subunit which proved to be dispensable for Ni binding, suggesting that the remaining three cysteines that are arranged in a plane are the major donors for Ni ligation.

An exchange of Asp456 in HoxH led to the formation of catalytically inactive SH which contained only a residual amount of Ni in the HoxH subunit. The distance between the carboxyl group of the corresponding Asp528 in the *D. gigas* hydrogenase (Figure 4) and the Ni atom is approximately 8 Å. Nevertheless, the aspartate is close to the cysteines in motif L5, and a structural reorganization of the molecule during NiFe cofactor insertion and C-terminal processing has been discussed (*17*). Therefore, we propose that Asp456 in HoxH is directly involved in the maturation of the NiFe center.

The five remaining mutant proteins were shown to contain Ni, indicating that metal insertion was not disturbed. Nevertheless, our data clearly demonstrate that these conserved residues are without exception important for the function of the SH protein. An alteration of Arg60 in HoxH had the most severe effect; the resulting mutant protein failed to form the tetramer. The corresponding Arg63 residue of the crystal structure is placed at the interface between the large and the small subunit close to the proximal [4Fe-4S] cluster (Figure 4). Therefore, we conclude that in the HoxH-[R60L] mutant protein the contact with the subunit HoxY is affected. The lack of any H_2-activating function in this mutant is consistent with previous results showing that the smallest catalytically active hydrogenase unit is the dimer (*8*).

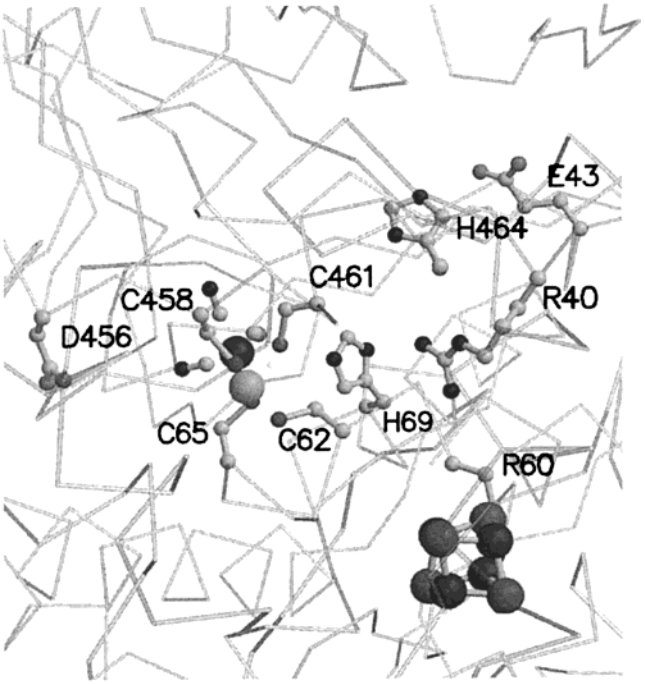

FIGURE 4: Closeup view of the hydrogen active site of the [NiFe] hydrogenase from *D. gigas* (*17*, *18*). The coordinates (2frv) were taken from the Brookhaven Protein Data Bank. Side chains of conserved amino acids, the NiFe center with three diatomic ligands, and the proximal [4Fe-4S] are shown in ball-and-stick representations in which the metal atoms and the acid-labile sulfur atoms are emphasized as large balls. The C_α backbones of the large and small subunit are represented by lines. For the purpose of orientation, the residue numbering of *A. eutrophus* HoxH is adopted here, and the numbers of the *D. gigas* hydrogenase are given in parentheses: R40 (R43), E43 (E46), R60 (R63), C62 (C65), C65 (C68), H69 (H72), D456 (D528), C458 (C530), C461 (C533), and H464 (H536). The figure was prepared using Molscript (*47*).

An important aspect in hydrogenase catalysis is the disposal of protons and the transfer of electrons. A set of histidines and a partially exposed glutamate of motifs L1, L2, and L5 have been initially proposed for the transfer of protons from the active site of the *D. gigas* hydrogenases to the solvent medium (*17*). Although the proposed proton-transfer pathway needs some modification due to an error in the original nucleotide sequence, which incorrectly predicted a nonconserved histidine residue, a proton transferring function of the conserved glutamate and histidine residues is still a viable consideration (*2*). The structure of the enzyme from *Desulfovibrio vulgaris* strain Miyasaki F revealed a Mg atom in the large subunit, coordinated by the glutamate of motif L1 and the histidine of L5 (*19*). The function of the Mg is not known. SH mutant proteins modified in corresponding residues of this region (Glu43, His69, and His464; see Figure 4) were identified as Ni-containing tetrameric proteins. The loss of at least 75% of the D_2-H^+ exchange activity is in line with the hypothesis that these mutant proteins are affected in proton transfer.

Since this activity depends on proton exchange, H^+ transferring functions seem not to be completely blocked.

The final most interesting mutant protein, HoxH[R40L], shares some properties assigned to the putative proton-transfer-deficient group. It is formed as a Ni-containing tetrameric protein, which exhibits a high level of D_2-H^+ exchange activity but is completely devoid of H_2:acceptor oxidoreductase function. This result shows that the mutant protein is still capable of binding and cleaving D_2 and exchanging D^+ with solvent protons. The crystal structure of the *D. gigas* enzyme illustrates that the corresponding Arg43 is facing the space between the NiFe center and the proximal [4Fe-4S] cluster (Figure 4) (*17*). The NH1 group of the arginine side chain is 5.3 Å from the C_β atom of Cys65, a terminal cysteine ligand of the Ni, and the NH2 group is 3.7 Å from the C_β atom of Cys17, a cysteine ligand of the proximal cluster in the small subunit. These two cysteines are on the axis between the Ni and the proximal [4Fe-4S] cluster and could be involved in electron transfer (*17*). Furthermore, a ligand-based redox chemistry in the hydrogen active site was proposed (*1*, *48*). Dole et al. (*26*) favors the terminal cysteines of the Ni being directly involved in H_2 oxidation. The positively charged and strictly conserved arginine may play an active role in the catalytic redox cycle at the stage of hydride oxidation by providing an efficient transfer of electrons from the active site to the connecting cluster or by providing a catalytic proton-transfer reaction.

The mutant analysis presented in this study is a straightforward molecular approach contributing to the understanding of the catalytic mechanism of [NiFe] hydrogenases. The mutant proteins are promising tools for future more sophisticated biochemical and spectroscopic investigations.

ACKNOWLEDGMENT

We thank Dr. V. M. Fernandez for his encouriging help during the D_2-H^+ exchange measurements in his laboratory. We are indebted to A. Strack for expert technical assistance, Dr. S. P. J. Albracht for valuable suggestions and stimulating discussions about the manuscript, and Dr. N. Sträter for his help using the program Molscript.

REFERENCES

1. Albracht, S. P. J. (1994) *Biochim. Biophys. Acta 1188*, 167−204.
2. Frey, M. (1998) *Struct. Bonding (Berlin) 90*, 98−124.
3. Bowien, B., and Schlegel, H. G. (1981) *Annu. Rev. Microbiol. 35*, 405−452.
4. Schink, B., and Schlegel, H. G. (1979) *Biochim. Biophys. Acta 567*, 315−324.
5. Bernhard, M., Benelli, B., Hochkoeppler, A., Zanoni, D., and Friedrich, B. (1997) *Eur. J. Biochem. 248*, 179−186.
6. Schneider, K., and Schlegel, H. G. (1976) *Biochim. Biophys. Acta 452*, 66−80.
7. Friedrich, B., and Schwartz, E. (1993) *Annu. Rev. Microbiol. 47*, 351−383.
8. Massanz, C., Schmidt, S., and Friedrich, B. (1998) *J. Bacteriol. 180*, 1023−1029.
9. Schneider, K., Cammack, C., and Schlegel, H. G. (1984) *Eur. J. Biochem. 142*, 75−84.
10. Walker, J. E. (1992) *Q. Rev. Biophys. 25*, 253−324.
11. Friedrich, T., and Weiss, H. (1997) *J. Theor. Biol. 187*, 529−540.
12. Tran-Betcke, A., Warnecke, U., Böcker, C., Zaborosch, C., and Friedrich, B. (1990) *J. Bacteriol. 172*, 2920−2929.
13. Kortlüke, C., and Friedrich, B. (1992) *J. Bacteriol. 174*, 6290−6293.
14. Voordouw, G. (1992) *Adv. Inorg. Chem. 38*, 397−422.
15. Eidsness, M. K., Scott, R. A., Pickrill, B., DerVartanian, D. V., Le Gall, J., Moura, I., Moura, J. J. G., and Peck, H. D., Jr. (1989) *Proc. Natl. Acad. Sci. U.S.A. 86*, 147−151.
16. Sorgenfrei, O., Klein, A., and Albracht, S. P. J. (1993) *FEBS Lett. 332*, 291−297.
17. Volbeda, A., Charon, M.-H., Piras, C., Hatchikian, E. C., Frey, M., and Fontecilla-Camps, J. C. (1995) *Nature 373*, 580−587.
18. Volbeda, A., Garcin, E., Piras, C., de Lacey, A. L., Fernandez, V. M., Hatchikian, E. C., Frey, M., and Fontecilla-Camps, J. C. (1996) *J. Am. Chem. Soc. 118*, 12989−12996.
19. Higuchi, Y., Yagi, T., and Yasuoka, N. (1997) *Structure 5*, 1671−1680.
20. Montet, Y., Amara, P., Volbeda, A., Vernede, X., Hatchikian, E. C., Field, M. J., Frey, M., and Fontecilla Camps, J. C. (1997) *Nat. Struct. Biol. 4*, 523−526.
21. Bagley, K. A., van Garderen, C. J., Chen, M., Duin, E. C., Albracht, S. P. J., and Woodruff, W. H. (1994) *Biochemistry 33*, 4980−4993.
22. Happe, R. P., Roseboom, W., Bagley, K. A., Pierik, A. J., and Albracht, S. P. J. (1997) *Nature 385*, 126.
23. de Lacey, A. C., Hatchikian, E. C., Volbeda, A., Frey, M., Fontecilla-Camps, J. C., and Fernandez, V. M. (1997) *J. Am. Chem. Soc. 119*, 7181−7189.
24. Van der Spek, T. M., Arendsen, A. F., Happe, R. P., Yun, S., Bageley, K. A., Stufkens, D. J., Hagen, W. R., and Albracht, S. P. J. (1996) *Eur. J. Biochem. 237*, 629−634.
25. Friedrich, B., Bernhard, M., Dernedde, J., Eitinger, T., Lenz, O., Massanz, C., and Schwartz, E. (1996) in *Microbial Growth on C1 Compounds* (Lindstrom, M. E., and Tabita, F. R., Eds.) pp 110−117, Kluwer Academic Publishers, Dordrecht, The Netherlands.
26. Dole, F., Fournel, A., Margo, V., Hatchikian, E. C., Bertrand, P., and Guigliarelli, B. (1997) *Biochemistry 36*, 7847−7854.
27. Pavlov, M., Siegbahn, P. E. M., Blomberg, M. R. A., and Crabtree, R. H. (1998) *J. Am. Chem. Soc. 120*, 548−555.
28. Krasna, A. I., and Rittenberg, D. (1954) *J. Am. Chem. Soc. 76*, 3015−3020.
29. Massanz, C., Fernandez, V. M., and Friedrich, B. (1997) *Eur. J. Biochem. 245*, 441−448.
30. Simon, R., Priefer, U., and Pühler, A. (1983) *Bio/Technology 1*, 717−774.
31. Lenz, O., Schwartz, E., Dernedde, J., Eitinger, M., and Friedrich, B. (1994) *J. Bacteriol. 176*, 4385−4393.
32. Friedrich, B., Heine, E., Fink, A., and Friedrich, C. G. (1981) *J. Bacteriol. 145*, 1144−1149.
33. Miller, J. H. (1972) *Experiments in molecular genetics*, Cold Spring Harbor Laboratory Press, Cold Spring Harbor, NY.
34. Sambrook, J., Fritsch, E. F., and Maniatis, T. (1989) *Molecular cloning: a laboratory manual*, 2nd ed., Cold Spring Harbor Laboratory Press, Cold Spring Harbor, NY.
35. Mikaelian, I., and Sergant, J. (1992) *Nucleic Acids Res. 20*, 376.
36. Eberz, G., Hogrefe, C., Kortlüke, C., Kamienski, A., and Friedrich, B. (1986) *J. Bacteriol. 168*, 636−641.
37. Lowry, O. H., Rosebrough, N. J., Farr, A. L., and Randall, R. J. (1951) *J. Biol. Chem. 193*, 265−275.
38. Dernedde, J., Eitinger, T., Patenge, N., and Friedrich, B. (1996) *Eur. J. Biochem. 235*, 351−358.
39. Towbin, H., Staehlin, T., and Gordon, J. (1979) *Proc. Natl. Acad. Sci. U.S.A. 76*, 4350−4357.
40. Thiemermann, S., Dernedde, J., Bernhard, M., Schroeder, W., Massanz, C., and Friedrich, B. (1996) *J. Bacteriol. 178*, 2368−2374.
41. Cammack, R., Fernandez, V. M., and Hatchikian, E. C. (1994) *Methods Enzymol. 234*, 43−68.
42. Maier, T., and Böck, A. (1996) *Adv. Inorg. Biochem. 11*, 173−192.

43. Wolf, I., Buhrke, T., Dernedde, J., Pohlmann, A., and Friedrich, B. (1996) *Arch. Microbiol. 170*, 451−459.
44. Sayavedra-Soto, L. A., and Arp, D. J. (1993) *J. Bacteriol. 175*, 3414−3421.
45. Rousset, M., Montet, Y., Guigliarelli, B., Forget, N., Asso, M., Bertrand, P., Fontecilla-Camps, J. C., and Hatchikian, E. C. (1998) *Proc. Natl. Acad. Sci. U.S.A. 85*, 11625−11630.
46. Przybyla, A. E., Robbins, J., Menon, N., and Peck, H. D. J. (1992) *FEMS Microbiol. Rev. 88*, 109−136.
47. Kraulis, P. J. (1991) *J. Appl. Crystallogr. 24*, 946−950.
48. Choudhury, S. B., Pressler, M. A., Mirza, S. A., Day, R. O., and Maroney, M. J. (1994) *Inorg. Chem. 33*, 4931−4839.

BI9908080